NIH Public Access
Author Manuscript
J Am Chem Soc. Author manuscript; available in PMC 2010 December 9.

Published in final edited form as:
J Am Chem Soc. 2009 December 9; 131(48): 17591–17596. doi:10.1021/ja9049355.

Hyperpolarized [2-^{13}C]-Fructose: A Hemiketal DNP Substrate for *In Vivo* Metabolic Imaging

Kayvan R. Keshari[a,b], **David M. Wilson**[a], **Albert P. Chen**[c], **Robert Bok**[a], **Peder E. Z. Larson**[a], **Simon Hu**[a], **Mark Van Criekinge**[a], **Jeffrey M. Macdonald**[b], **Daniel B. Vigneron**[a], and **John Kurhanewicz**[a,*]

[a] Department of Radiology and Biomedical Imaging, University of California San Francisco (UCSF), 1700 4th St., Byers Hall 203, San Francisco, California, United Sates 94158

[b] Department of Biomedical Engineering, University of North Carolina Chapel Hill (UNC), 152 MacNider Hall, Campus Box 7575, Chapel Hill, North Carolina, United States 27599

[c] GE Healthcare, 333 Ravenswood Ave., Building 207, Menlo Park, CA 94025

Abstract

Hyperpolarized ^{13}C labelled molecular probes have been used to investigate metabolic pathways of interest as well as facilitate *in vivo* spectroscopic imaging by taking advantage of the dramatic signal enhancement provided by DNP. Due to the limited lifetime of the hyperpolarized nucleus, with signal decay dependant on T_1 relaxation, carboxylate carbons have been the primary targets for development of hyperpolarized metabolic probes. The use of these carbon nuclei makes it difficult to investigate upstream glycolytic processes, which have been related to both cancer metabolism as well as other metabolic abnormalities, such as fatty liver disease and diabetes. Glucose carbons have very short T_1s (< 1 sec) and therefore cannot be used as an *in vivo* hyperpolarized metabolic probe of glycolysis. However, the pentose analogue fructose can also enter glycolysis through its phosphorylation by hexokinase and yield complimentary information. The C_2 of fructose is a hemiketal that has a relatively longer relaxation time (≈ 16 s at 37° C) and high solution state polarization (≈ 12%). Hyperpolarized [2-^{13}C]-fructose was also injected into a transgenic model of prostate cancer (TRAMP) and demonstrated difference in uptake and metabolism in regions of tumor relative to surrounding tissue. Thus, this study demonstrates the first hyperpolarization of a carbohydrate carbon with a sufficient T_1 and solution state polarization for *ex vivo* spectroscopy and *in vivo* spectroscopic imaging studies.

Keywords

DNP; hyperpolarized carbon; hemiketal; fructose; metabolism

INTRODUCTION

Recent development of techniques to retain highly polarized spins in solution via dynamic nuclear polarization (DNP) has enabled hyperpolarized ^{13}C NMR spectroscopy and MR spectroscopic imaging studies with signal enhancements of over 10,000 fold in short

*Correspondence and Reprint Request: Professor John Kurhanewicz, UCSF Mission Bay Campus, Byers Hall, Room 203E, 1700 4th St, San Francisco, CA 94158-2330, Tel: (415) 514-9711, Fax: (415) 514-4714, John.Kurhanewicz@radiology.ucsf.edu.

SUPPORTING INFOMRATION: Supporting Information Available: The complete citation of reference [29] (Complete Ref. _) is available as well as the full CSI data spectral matrix for the studies corresponding to Figure 4 (Figure S1) and 5 (Figure S2). This material is available free of charge via the Internet at http://pubs.acs.org.

NIH-PA Author Manuscript
NIH-PA Author Manuscript
NIH-PA Author Manuscript

NIH-PA Author Manuscript

NIH-PA Author Manuscript

NIH-PA Author Manuscript

acquisition times [1,2]. This new technique has powerful applications for metabolic imaging of cancer. The *in-vivo* metabolism of [1-^{13}C]-pyruvate and its metabolic products, [1-^{13}C]-lactate, [1-^{13}C]-alanine and [^{13}C] bicarbonate, have been shown to correlate with disease progression [3] and response to therapy [4] in animal models. DNP substrates require a long T_1 relaxation to facilitate efficient spin diffusion during the process of hyperpolarization [5,6]. Carbonyl carbons, which lack attached protons and limit the relaxation as a result of dipolar cross relaxation, have been the standard species to label and polarize with T_1's on the order of 40–60 seconds, depending on the field strength [7–9].

Although a number of molecules of interest have been polarized and observed through their carbonyl carbons [1,3,9–11], a great number of important metabolic intermediates do not contain a carbonyl. Specifically, changes in carbohydrate metabolism occur with the evolution and progression of cancer [12–14] as well as a number of other human diseases such as non-alcoholic fatty liver disease [15–17]. Glucose carbons have very short T1s (< 1 sec) and therefore uniformly ^{13}C labelled glucose, a mainstay of current metabolic studies [18,19], cannot be used as an *in vivo* hyperpolarized metabolic probe of glycolysis.

Fructose, occurring as an isomeric mixture of five and six membered rings, has as its most stable isomer β-fructopyranose with a hemiketal in the C_2 position. Fructose can enter glycolyis via hexokinase or fructokinase [20–24]. The one-step metabolism via hexokinase to the phosphorylated fructose-6-phosphate is analogous to the first step of glycolysis, in which glucose is phosphorylated to glucose-6-phosphate. The metabolic flux to fructose-6-phosphate in the cell is related to the downstream glycolytic metabolic events as well as activity of the pentose phosphate pathway (PPP) [25–27]. The pentose phosphate pathway is responsible for the predominant amount of nucleotide synthesis (which is increased at high turnover rates) and has been postulated to be a source of regeneration of NADPH in cancer cells [14] making them more resistant to oxidative stress and allowing them to replenish glutathione.

Furthermore, metabolism of fructose is implicated in non-alcoholic steatohepatitis (NASH) [15], and in the pathogenesis of specific types of cancer. Fructose can also be metabolized to the fructose-1-phosphate via fructokinase, a reaction that takes place primarily in the liver [20]. Hepatic uptake is via the GLUT5 transporter, that demonstrates relative specificity for fructose. Expression of this transporter may be an important biomarker for disease in extrahepatic tissues. For example, the human fructose transporter, GLUT5 (as shown in Figure 1), is highly expressed in breast cancer cell lines but not by normal breast tissue [28]. A recent study of metabolites in the prostate gland has also shown a relationship between fructose and benign versus cancer tissues [29]. Thus the goal of this study was to investigate a new non-carbonyl hyperpolarized ^{13}C probe, [2-^{13}C]-fructose for the study of metabolism *in vivo*.

MATERIALS AND METHODS

Hyperpolarized [2-^{13}C]-Fructose

A 4.0M solution of [2-^{13}C]-fructose (Isotec, Miamisburg, OH) in water containing 15mM OX063 trityl radical (Oxford Instruments) was hyperpolarized on a Hypersense instrument (Oxford Instruments) as previously described [1]. The frozen sample was dissolved in 1X phosphate buffered saline (PBS), with a resultant pH of 7.6, and transferred immediately to a 10mm NMR tube.

11.7T NMR Studies

NMR studies were performed on an 11.7T Varian INOVA spectrometer (125MHz ^{13}C, Varian Instruments) using a 10mm ^{15}N/^{31}P/^{13}C broadband direct detect probe and temperature controlled at 37°C. Initially, a thermal spectrum was acquired for a natural abundance fructose

NIH-PA Author Manuscript

NIH-PA Author Manuscript

NIH-PA Author Manuscript

sample in 1X PBS buffer at 37°C (nt=9000, sw=30000, np=30000, TR=3.5s, acq time= 0.5s) using a 45-degree pulse. Figure 2 demonstrates the natural abundance ^{13}C spectrum of fructose. The C_2 carbon resonances are denoted by the blue brackets and correspond to the isomeric distribution of the two ring forms (pyranose and furanose forms) of the fructose molecule. For the acquisition of hyperpolarized ^{13}C spectra eighty pulse and acquire hyperpolarized ^{13}C NMR spectra (1 scan, spectral window = 20000 Hz, number of points= 40000, TR=3s, total acquisition time = 2 min 55s) were acquired using a 5° pulse and proton decoupled using a waltz-16 decoupling scheme. Hyperpolarized studies were followed by acquisition of thermal data with nearly identical parameters, using a 90° flip angle and a repetition time of greater than four T_1's (TR=300s, nt=16). For T_1 measurements hyperpolarized solution was placed into a NMR tube pre-heated to 37° C and this temperature is maintained using the variable temperature unit of the NMR spectrometer. T_1's were determined by collecting a series of spectra with 3 sec temporal resolution, starting 12 secs after dissolution. These spectra were then fit to a mono-exponential function to determine the spin-lattice relaxation time as previously described[9,30,31]. Percent polarization in solution was calculated by comparing the first hyperpolarized spectrum acquired with its thermal spectrum, correcting for differences in tip angle (5 versus 90), and the number of transients (1 versus 16) obtained. Solution state polarizations were calculated by correcting the enhancement for the T_1 relaxation during the transfer time (12 secs) from the polarizer to the spectrometer, and the thermal polarization at 11.7T (9.6 ppm).

For NMR studies of the enzymatic conversion of Fructose to fructose-6-phosphate, hyperpolarized [2-^{13}C]-fructose was reacted with 400U of hexokinase (Sigma Aldrich) in the presence of 15mM ATP, 50mM TRIS and 13mM $MgCl_2$. The labelling and mechanism for transport and metabolism is shown below (Figure 1), though in this enzymatic study the transport element has been removed and the enzyme activity was independently measured. Peaks corresponding to fructose-6-phosphate were identified using a natural abundance carbon spectrum, using a similar set of experimental parameters.

3T Studies

T_1 studies were performed using a 3T GE Signa™ scanner (GE Healthcare, Waukesha, WI) equipped with the MNS (multinuclear spectroscopy) hardware package similar to studies at 11.7T, with temperature maintained using a heating pad calibrated to 37°C. Solution spectra were acquired using a 5° non-localized pulse, TR=3s and fit to a mono-exponential. The RF coil used in these experiments was a dual-tuned ^{1}H-^{13}C coil with a quadrature ^{13}C channel and linear ^{1}H channel construction based on an earlier design and also used in ^{13}C-pyruvate mouse imaging studies. For animal studies, T_2-weighted fast spin echo images were acquired prior to MRSI studies to denote anatomy and place voxels on the region of interest. *In vivo* MRSI studies were carried out using a compressed sensing double spin 3D MRSI acquisition scheme as previously published [32] with a TE = 140 ms, TR=215 ms, FOV = 8 cm × 8 cm, and 16 × 8 resolution. 500 μl of of 80 mM [2-^{13}C]-fructose (0.0013 mmols/kg) was injected similar to previously described methods for [1-^{13}C] pyruvate in a transgenic model of prostate cancer (TRAMP) [3]. High dose infusions of fructose (0.5g/kg) can lead to hyperuricemia[33], but this is well above the dose given in these studies (0.24mg/kg). These injections were compared to the standard [1-^{13}C]-pyruvate injection for the same voxel in a tumor region of interest. Maps of resonance distributions were generated from the peak heights in each voxel and overlaid on the corresponding T_2-weighted image.

RESULTS AND DISCUSSION

Calculated T_1's for the C_2 fructose carbon are tabulated in Table 1 for the cyclic isomers of fructose (β-fructofuranose, β-fructopyranose, α-fructofuranose) at both 11.7T and 3T, the field

NIH-PA Author Manuscript

NIH-PA Author Manuscript

NIH-PA Author Manuscript

stenghts of the *ex vivo* and *in vivo* hyperpolarized studies. The open chain (linear) isomer of fructose is present in very small amounts (0.4%) [21,34] and not observed in the hyperpolarized NMR spectra. There was no significant difference in the C_2 T_1 between the cyclic isomers of fructose, most likely due to the fast chemical of the isomeric forms [34]. There was a small decrease in T_1 relaxation (≈ 2 sec) of the C_2 carbon with decreasing magnetic field strength from 11.7T to 3T (Table 1). To date, hyperpolarized ^{13}C agents have involved labelling at carbonyl positions, such as the C_1 position of pyruvate, due to their relatively long T_1's [1,2,7,9,30,35]. In contrast to the quaternary hemiketal carbon of the fructose isomers, carbonyl carbons decrease in T_1 with increasing field strengths[36]. This difference is predominantly due to chemical shift anisotropy dominating the T_1 relaxation of carbonyl carbons at higher field strengths[36]. This does not hold for the hemiketal of fructose, leading to the typical lengthening of T_1 with increasing field strength. Percent polarizations (Table 1) show similar values for the isomers of fructose with an average solution state polarization at 37° C of 12%. These polarization values are comparable, although somewhat lower, than those reported for other compounds of interest[1,37,38] such as pyruvate which has been reported to be polarized from 21–30%[3,39]. There was no T_1 dependence on pH observed for pH ranges 5.9–7.8 for the fructose isomers.

The polarization levels were calculated relative to thermal signals from the same sample. The DNP polarizer sits in the fringe field of the 11.7T spectrometer in order to eliminate the possibility of passing the hyperpolarized sample through a zero field and loosing all polarization. For carbonyls such as the C_1 of pyruvate, we know that the T_1 at lower magnetic field strengths, and that the T_1 in the fringe field of the magnet should be longer, on the order of 80 secs as compared to 52 secs at 11.7T. This is due to the relationship between CSA and field strength ($CSA1B_0$ [2]), which dominates the carbonyl T_1 at high field strengths [36]. However, as demonstrated in this publication, the T_1 of the quaternary C_2 carbon of fructose is only slightly longer at higher field strengths (Table 1). Therefore the T_1 in the fringe field should be slightly shorter than 3T, which would result in a small underestimation of the % polarization at time zero.

The reaction of hyperpolarized C_2-fructose with hexokinase after addition of fructose to the hexokinase in buffer within the NMR yields the phosphorylated pentose within 5 seconds (Figure 3). An expansion of the downfield region of the spectrum (Figure 3a) shows the split in the 105.5ppm resonance, which is a combination of both the β-fructofuranose and the β-fructofuranose-6-phosphate (the predominant isomeric form of fructose-6-phosphate). Figure 3 also compares the first scan of the hyperpolarized acquisition (Figure 3b) versus the thermal spectrum acquired over 85 minutes post DNP (Figure 3c). It is apparent that the enzyme has now fully converted the fructose to fructose-6-phosphate and there is no longer a resonance corresponding to β-fructopyranose.

Figure 4 demonstrates the metabolism following separate injections of 80mM hyperpolarized fructose (Figure 4d) and pyruvate (Figure 4e) in the same TRAMP mouse. As previously published (3), the primary TRAMP tumor demonstrates high levels of hyperpolarized lactate, as well good signal to noise spectra of hyperpolarized fructose and it's metabolite β-fructofuranose-6-phosphate. Injections of 80mM hyperpolarized fructose yielded an average total signal-to-noise ratio of 21.0 ± 2.1 in tumor slices (an average of 70 voxels in 2 slices was used for N=3 TRAMP mice). Because the isomeric ratio of the fructose pyranose to furanose in solution is approximately 77/23 [21] the *in vivo* peak at 105.5ppm (and if visible the downstream 108.25ppm resonance) is not solely due to β-fructofuranose-6-phosphate but also has a small contribution from β-fructofuranose. In this relatively large TRAMP tumor, both high levels of LDH activity and hexokinase activity were observed 15 secs post-injection in the same 0.035cc voxels. Figure 4b demonstrates the distribution of the total fructose signal throughout the slice, a measure of combined delivery and uptake of hyperpolarized Fructose.

NIH-PA Author Manuscript

NIH-PA Author Manuscript

NIH-PA Author Manuscript

Slightly higher levels of total hyperpolarized fructose were observed in the tumor region relative to surrounding muscle in the same slice. In comparison, Figure 4c demonstrates the distribution of the resonance at 105.5ppm, which includes the metabolite β-fructofuranose-6-phosphate. Importantly, this resonance has a good signal-to- noise (≈ 5:1) and is co-localized in regions of high lactate within the tumor (Figures 4d and 4e).

Figure 5 demonstrates a case where there was tumor only in the left side of the murine prostate, providing a direct comparison of hyperpolarized fructose uptake/delivery and metabolism between benign and malignant prostate tissues. The MRSI data demonstrated that the resonance corresponding to the composite β-fructofuranose and β-fructofuranose-6-phosphate were higher in the regions of tumor as compared to the benign prostate tissues (Figure 5d). Interestingly, there is no difference in total hyperpolarized fructose in regions of malignant versus benign prostate tissue. However, the composite β-fructofuranose and β-fructofuranose-6-phosphate resonance (Figure 5c) was higher in malignant left lobe of the prostate as compared to the benign right side (Figure 5c and d).

CONCLUSION

In this study, [2-^{13}C]-fructose was hyperpolarized using the DNP method and shown to have sufficiently long T_1's and polarizations sufficient for hyperpolarized ^{13}C NMR spectroscopic and MRSI studies. The hemiketal C_2 of fructose demonstrates the first non-carbonyl to be hyperpolarized for use as a metabolic probe and suggests the potential of using other hyperpolarized probes involving quaternary carbons even those in ring structure. Enzymatic conversion of hyperpolarized [2-^{13}C]-fructose, to fructose-6-phosphate has been demonstrated *in vitro* and *in vivo*. While the composite β-fructofuranose and β-fructofuranose-6-phosphate resonance was associated with tumor regions, it was also present in some surrounding benign tissues, and additional studies are necessary to fully understand the composition of this resonance and its relationship to malignancy. The enzymatic conversion of hyperpolarized fructose allows the probing of important changes in glycolytic metabolism upstream of pyruvate, including upregulated hexose uptake [28], hexokinase activity and changes in flux through the pentose phosphate pathway [14]. Although, this study was focused on prostate cancer models, upstream glyolytic processes have been the basis of a number of cancer studies including the HIF-1 and PI3K related processes [14]. Therefore changes in fructose metabolism may be important in the assessment of therapies that target these pathways. A potential link between fructose metabolism and non-alcoholic fatty liver disease has also been demonstrated [40] and thus hyperpolarized fructose could become a valuable metabolic imaging agent to study this and other diseases both *ex vivo* and *in vivo*. Moreover, the dose of fructose given in this murine study translates into a very safe patient dose.

Supplementary Material

Refer to Web version on PubMed Central for supplementary material.

Acknowledgments

The authors would like to acknowledge the following funding mechanisms for supporting this research: National Institutes of Health (R21 EB005363, R01 EB007588 R21 GM075941) and NIBIB T32 Training Grant 1 T32 ED001631.

Grant sponsors: National Institutes of Health (R21 EB005363, R01 EB007588); NIBIB T32 Training Grant 1 T32 ED001631

NIH-PA Author Manuscript

NIH-PA Author Manuscript

NIH-PA Author Manuscript

References

1. Ardenkjaer-Larsen JH, Fridlund B, Gram A, Hansson G, Hansson L, Lerche MH, Servin R, Thaning M, Golman K. Proc Natl Acad Sci USA 2003;100:10158–10163. [PubMed: 12930897]
2. Golman K, Zandt RI, Lerche MH, Pehrson R, Ardenkjaer-Larsen JH. Cancer Res 2006;66:10855–10860. [PubMed: 17108122]
3. Albers MJ, Bok R, Chen AP, Cunningham CH, Zierhut ML, Zhang VY, Kohler SJ, Tropp J, Hurd RE, Yen YF, Nelson SJ, Vigneron DB, Kurhanewicz J. Cancer Res 2008;68:8607–8615. [PubMed: 18922937]
4. Day SE, Kettunen MI, Gallagher FA, Hu DE, Lerche M, Wolber J, Golman K, Ardenkjaer-Larsen JH, Brindle KM. Nat Med 2007;13:1382–1387. [PubMed: 17965722]
5. Abragam A, Goldman M. Rep Prog Phys 1978:41.
6. Borghini M. Physical Review Letters 1968;20:419–421.
7. Chen AP, Kurhanewicz J, Bok R, Xu D, Joun D, Zhang V, Nelson SJ, Hurd RE, Vigneron DB. Magnetic resonance imaging 2008;26:721–726. [PubMed: 18479878]
8. Merritt ME, Harrison C, Storey C, Jeffrey FM, Sherry AD, Malloy CR. Proc Natl Acad Sci USA 2007;104:19773–19777. [PubMed: 18056642]
9. Wilson DM, Hurd RE, Keshari KR, Van Criekinge M, Chen AP, Nelson SJ, Vigneron DB, Kurhanewicz J. Proc Natl Acad Sci USA. 2009
10. Schroeder MA, Atherton HJ, Ball DR, Cole MA, Heather LC, Griffin JL, Clarke K, Radda GK, Tyler DJ. The FASEB Journal. 2009
11. Warren WS, Jenista E, Branca RT, Chen X. Science 2009;323:1711–1714. [PubMed: 19325112]
12. Denko NC. Nat Rev Cancer. 2008
13. Ganapathy V, Thangaraju M, Prasad PD. Pharmacol Ther. 2008
14. Kroemer G, Pouyssegur J. Cancer Cell 2008;13:472–482. [PubMed: 18538731]
15. Farrell G, Larter C. Hepatology 2006;43:S99–S112. [PubMed: 16447287]
16. Huynh M, Luiken JJ, Coumans W, Bell R. Obesity (Silver Spring) 2008;16:1755–1762. [PubMed: 18483476]
17. Douard V, Ferraris RP. Am J Physiol Endocrinol Metab 2008;295:E227–237. [PubMed: 18398011]
18. Antoniewicz MR, Kelleher JK, Stephanopoulos G. Metab Eng 2006;8:324–337. [PubMed: 16631402]
19. Lane AN, Fan TW, Higashi RM, Tan J, Bousamra M, Miller DM. Experimental and Molecular Pathology 2009;86:165–173. [PubMed: 19454273]
20. Bais R, James HM, Rofe AM, Conyers RA. Biochem J 1985;230:53–60. [PubMed: 2996495]
21. Skoog M, Johansson G, Olsson B, Appelqvist R. Mikrochimica Acta 1988;III:131–142.
22. Funari V, Herrera V, Freeman D, Tolan D. Molecular Brain Research 2005;142:115–122. [PubMed: 16266770]
23. Petersen A, Kappler F, Szwergold BS, Brown TR. Biochem J 1992;284(Pt 2):363–366. [PubMed: 1599419]
24. Levi J, Cheng Z, Gheysens O, Patel M, Chan CT, Wang Y, Namavari M, Gambhir SS. Bioconjug Chem 2007;18:628–634. [PubMed: 17444608]
25. Voet, D.; Voet, JG. Biochemistry. Vol. 3. J. Wiley & Sons; New York: 2004.
26. Tong X, Zhao F, Thompson CB. Curr Opin Genet Dev 2009;19:32–37. [PubMed: 19201187]
27. Vizán P, Alcarraz-Vizán G, Díaz-Moralli S, Solovjeva O, Frederiks W, Cascante M. Int J Cancer 2009;124:2789–2796. [PubMed: 19253370]
28. Zamora-León SP, Golde DW, Concha II, Rivas CI, Delgado-López F, Baselga J, Nualart F, Vera JC. Proc Natl Acad Sci USA 1996;93:1847–1852. [PubMed: 8700847]
29. Sreekumar A, et al. Nature 2009;457:910–914. [PubMed: 19212411]
30. Gallagher FA, Kettunen MI, Day SE, Lerche M, Brindle KM. Magnetic resonance in medicine: official journal of the Society of Magnetic Resonance in Medicine/Society of Magnetic Resonance in Medicine 2008;60:253–257. [PubMed: 18666104]
31. Golman K, Ardenkjaer-Larsen JH, Petersson JS, Mansson S, Leunbach I. Proc Natl Acad Sci USA 2003;100:10435–10439. [PubMed: 12930896]

NIH-PA Author Manuscript

NIH-PA Author Manuscript

NIH-PA Author Manuscript

32. Hu S, Lustig M, Chen AP, Crane J, Kerr A, Kelley DA, Hurd R, Kurhanewicz J, Nelson SJ, Pauly JM, Vigneron DB. J Magn Reson 2008;192:258–264. [PubMed: 18367420]
33. Wang YM, van Eys J. Annu Rev Nutr 1981;1:437–475. [PubMed: 6821187]
34. Goux WJ. Journal of the American Chemical Society 1985;107:4320–4327.
35. Gallagher FA, Kettunen MI, Day SE, Hu DE, Ardenkjaer-Larsen JH, in't Zandt R, Jensen PR, Karlsson M, Golman K, Lerche MH, Brindle KM. Nature 2008;453:940–U973. [PubMed: 18509335]
36. Ven, FJMvd. Multidimensional NMR in Liquids: Basic Principles and Experimental Methods. Wiley-VCH: New York; 1995. p. 356-358.
37. Merritt ME, Harrison C, Storey C, Sherry AD, Malloy CR. Magnetic resonance in medicine: official journal of the Society of Magnetic Resonance in Medicine/Society of Magnetic Resonance in Medicine 2008;60:1029–1036. [PubMed: 18956454]
38. Kohler SJ, Yen Y, Wolber J, Chen AP, Albers MJ, Bok R, Zhang V, Tropp J, Nelson SJ, Vigneron DB, Kurhanewicz J, Hurd RE. Magnetic resonance in medicine: official journal of the Society of Magnetic Resonance in Medicine/Society of Magnetic Resonance in Medicine 2007;58:65–69. [PubMed: 17659629]
39. Schroeder MA, Cochlin LE, Heather LC, Clarke K, Radda GK, Tyler DJ, Shulman RG. Proceedings of the National Academy of Sciences of the United States of America 2008;105:12051–12056. [PubMed: 18689683]
40. Donnelly KL, Smith CI, Schwarzenberg SJ, Jessurun J, Boldt MD, Parks EJ. J Clin Invest 2005;115:1343–1351. [PubMed: 15864352]

NIH-PA Author Manuscript

NIH-PA Author Manuscript

NIH-PA Author Manuscript

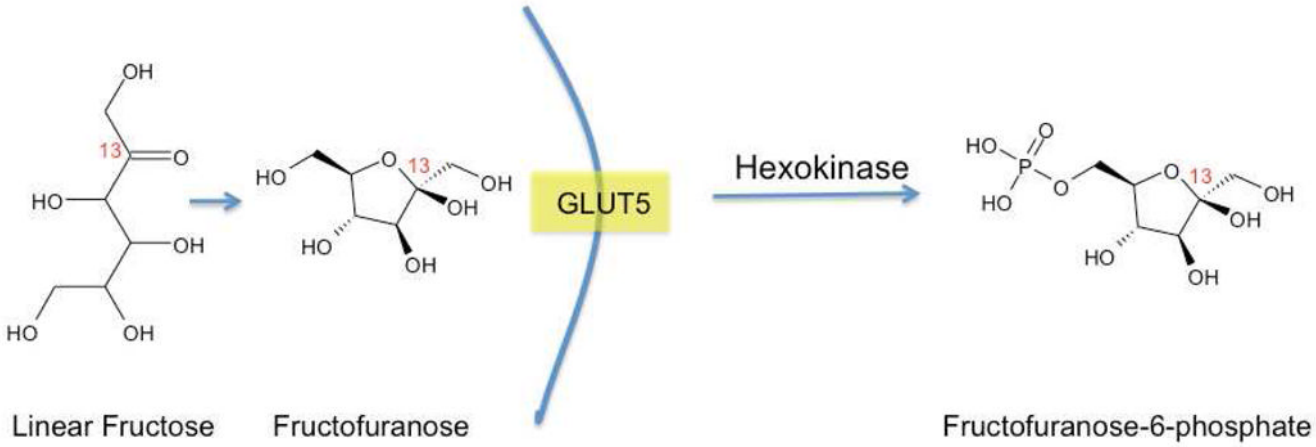

Figure 1.
The mechanism for transport by GLUT5 and the first step of metabolism of fructose to fructofuranose-6-phosphate by hexokinase.

NIH-PA Author Manuscript
NIH-PA Author Manuscript
NIH-PA Author Manuscript

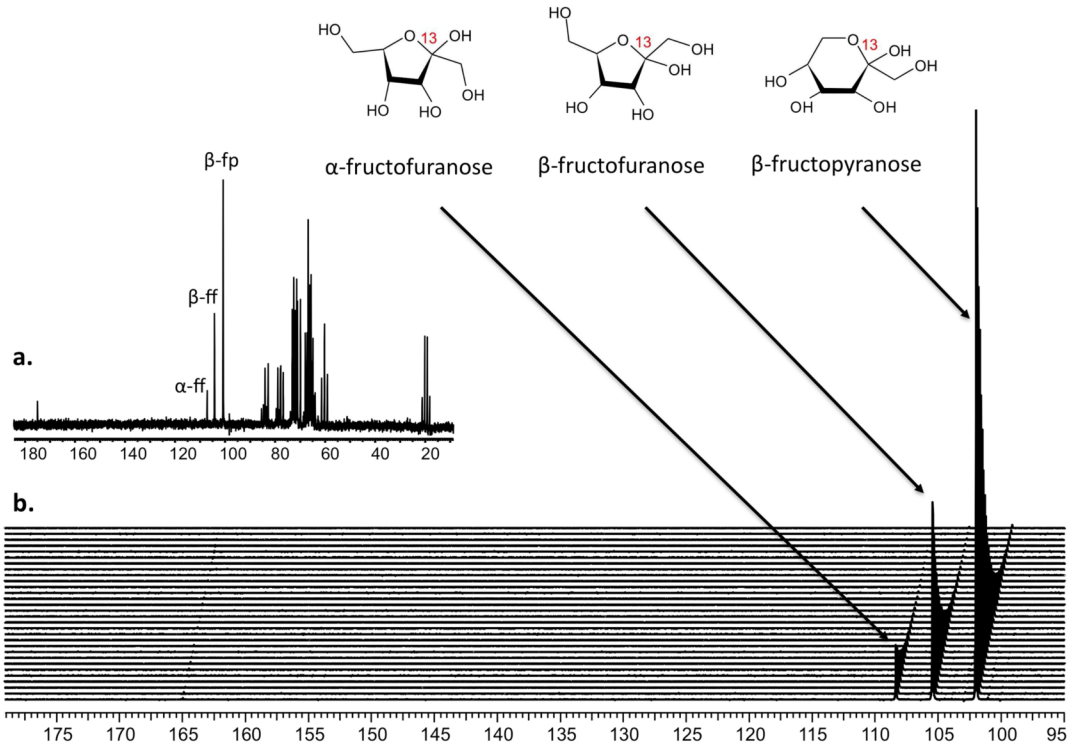

Figure 2.

The natural abundance spectrum of fructose (a) and DNP spectrum of [2-^{13}C]-fructose (b). The linear form is present in the DNP spectrum, but at a very low level analogous to the thermal spectrum. (Top) Structures of each of the isomers are shown with their analogous resonance.

NIH-PA Author Manuscript
NIH-PA Author Manuscript
NIH-PA Author Manuscript

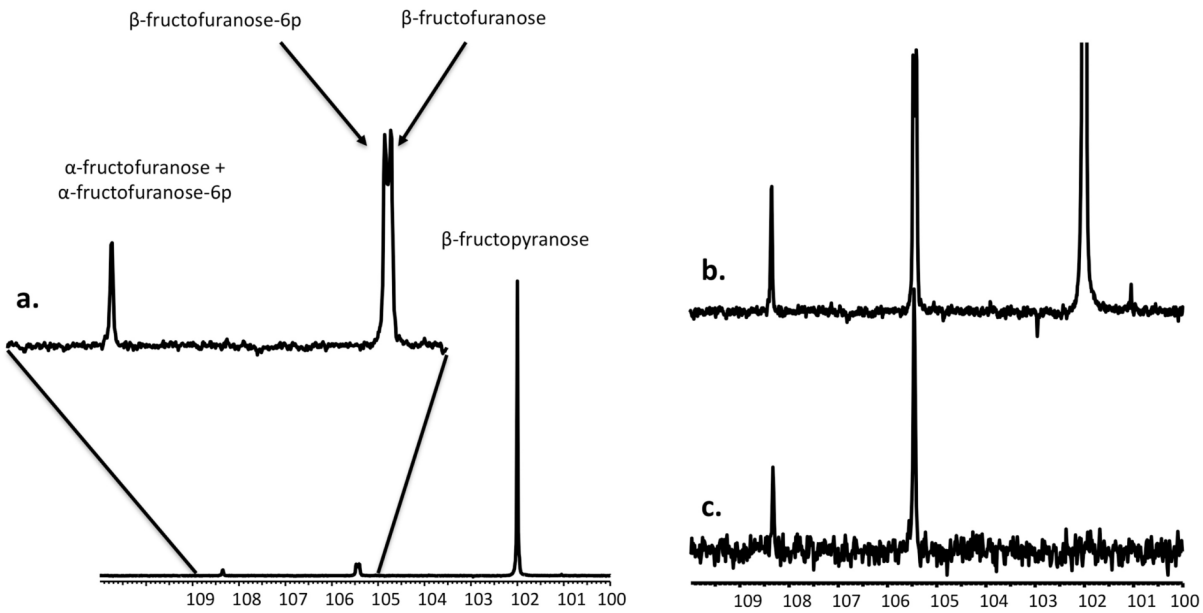

Figure 3.

(a) Spectrum of fructose reacted with 400U of hexokinase, the zoomed in region demonstrates the resonances corresponding to the fructose and fructose-6-phosphate. (b) The dynamic spectrum after 5 secs of reaction with hexokinase. (c) The thermal spectrum of same solution with hexokinase averaged 85 min post DNP.

NIH-PA Author Manuscript

NIH-PA Author Manuscript

NIH-PA Author Manuscript

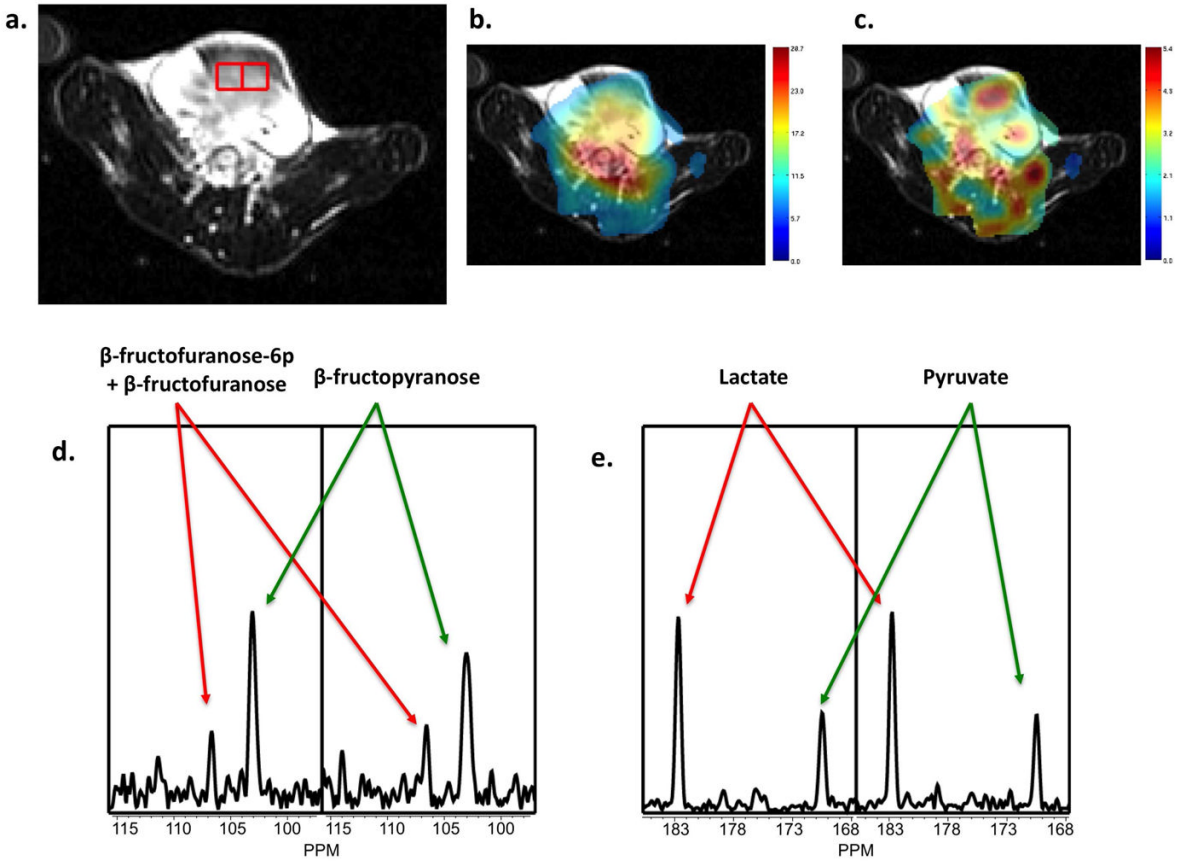

Figure 4.

(**a**) T_2-weighted image of a moderate to late stage TRAMP mouse prostate tumor. Metabolite image overlays of the resonances corresponding to total hyperpolarized fructose (**b**) and composite β-fructofuranose-6-phosphate and β-fructofuranose (**c**) obtained after injection of 80mM [2-^{13}C] fructose demonstrate spatial differences in total fructose versus the composite β-fructofuranose-6-phosphate resonance. Spectra corresponding to the two red voxels (**d**) in the tumor demonstrate the resonances corresponding to β-fructopyranose and the composite β-fructofuranose-6-phosphate and β-fructofuranose. Pyruvate and lactate resonances are shown from the same locations (**e**) obtained after an injection of 80mM hyperpolarized pyruvate in the same mouse.

NIH-PA Author Manuscript

NIH-PA Author Manuscript

NIH-PA Author Manuscript

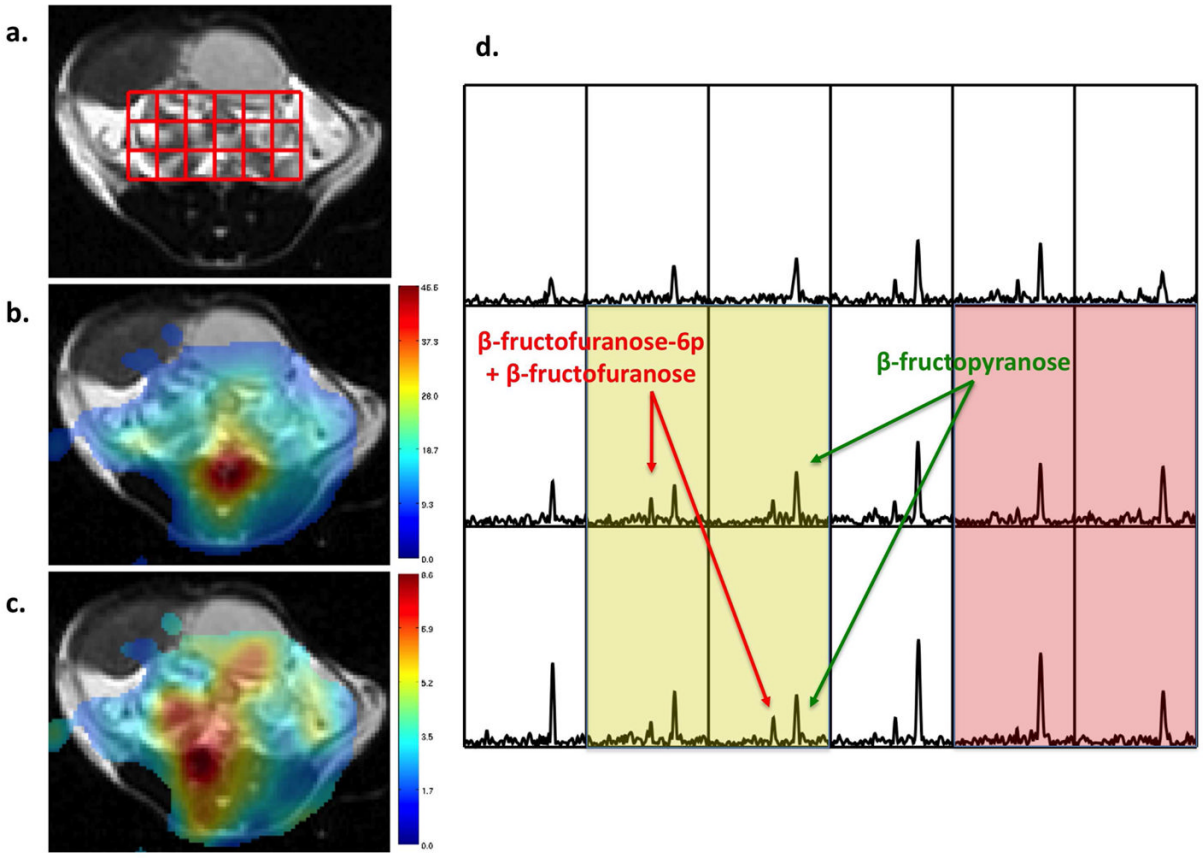

Figure 5.

(**a**) T_2-weighted image of a TRAMP mouse with tumor only on the right side of the prostate. Metabolic images of total hyperpolarized [2-^{13}C] fructose resonances (**b**) and the composite β-fructofuranose-6-phosphate and β-fructofuranose (**c**) are shown overlaid on the T_2 weighted image. Resonances corresponding to the β-fructopyranose and composite β-fructofuranose-6-phosphate and β-fructofuranose are shown in the corresponding spectral array (**d**). The yellow area demonstrates a region of tumor, compared to a region of benign prostate tissue in red. An unassigned spurious, low signal-to-noise resonance appears at 115 ppm.

NIH-PA Author Manuscript

NIH-PA Author Manuscript

NIH-PA Author Manuscript

Table 1

T_1 relaxation times at 11.7T and 3T (N=3 for both, ± s.d.) are shown for each of the isomers as well as percent polarization (N=3), which have been corrected for the time from dissolution to measurement. All studies were conducted at 37°C.

Isomer	T_1 sec (11.7T)	T_1 sec (3T)	%pol
β-fructopyranose	16.3 ± 0.5	14.5 ± 0.3	12.0 ± 2.2
β-fructofuranose	15.8 ± 0.5	13.4 ± 0.5	11.6 ± 2.5
α-fructofuranose	15.8 ± 0.5	13.4 ± 0.4	11.8 ± 2.0